PIb-01

Theoretical study of photoisomerization reaction between cyclohexadiene and hexatriene

Ayumi Ohta, Osamu Kobayashi, Toshimasa Ishida, and Shinkoh Nanbu
Faculty of Science and Technology, Sophia University, Kioicho, Chiyoda-ku, Tokyo 102-8554, Japan
e-mail address: o-ta.com@sophia.ac.jp

I.Introduction

Photoisomerization between 1,3-cyclohexadiene (CHD) and 1,3,5-*cis*-hexatriene (HT) has been attracting great interest as the model system of large-size photochromic molecules like diarylethenes. The isomerization process in both vapor and liquid phases has been experimentally investigated by several groups.

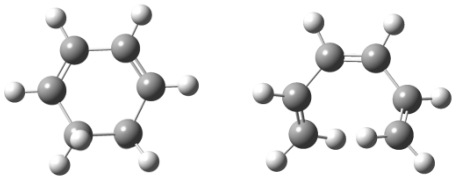

Figure.1 1,3-cyclohexadiene(left)
1,3,5-*cis*-hexatriene(right)

In this study, molecular dynamics (MD) for the photoisomerization of CHD in vapor phase was carried out with the full-dimensional model which consists of 42 degrees of freedom. The photoexcitation process from CHD was assumed to go along with Franck-Condon (FC) principle. The energy-relaxation processes after the photoexcitation to two excited states, S_1 and S_2, were explored by *ab initio* MD simulation. Since the main process of the nonradiative process would be governed by non-adiabatic transitions around pseudo-crossings of two potential curves, trajectory surface hopping (TSH) method with Zhu-Nakamura formula was employed to treat the non-adiabatic transition. The on-the-fly *ab initio* calculation was at complete active space 2nd perturbation (CASPT2) level with cc-pVDZ basis set. For the excitation to S_1 and S_2, 20 and 22 trajectory-computations were executed by our Intel XEON (Westmere, Nehalem, and Sandybridge cores) computers.

II. Result

Figure.2 is the typical trajectory decaying from S_2 in vapor phase. The product branching ratio of CHD to HT after photoexcitation to S_1 is found to be 60 : 40. The longest S_1-lifetime is 229 fs.

The ratio of CHD to HT after excitation to S_2 is 70 : 30; the photoisomerization prefers CHD product. The longest decay time to reach S_0 is 151 fs. This shorter lifetime than S_1 would be reasonable, because the excess energy is higher than the case of the transition to S_1, and moreover S_1 and S_2 states are lying close to each other.

On the other hand, the conformational feature when the non-adiabatic transition occurs is found to be quite similar in every case even for S_2-S_1 and S_1-S_0 transitions.

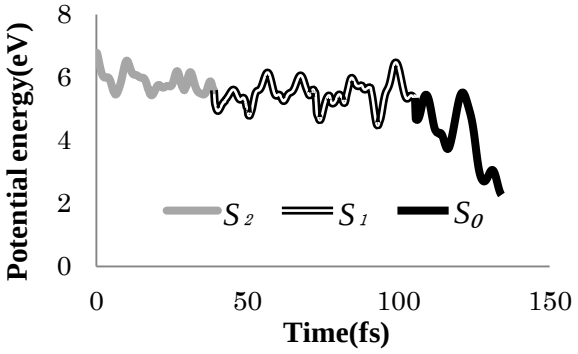

Figure.2 result of the typical trajectory in vapor phase

PIb-02

Theoretical study of cyclodextrins from gas phase to aqueous solution: intramolecular and intermolecular hydrogen bonding

Dai Akase and Misako Aida

Center for Quantum Life Science and Department of Chemistry, Graduate School of Science, Hiroshima University, 1-3-1 Kagamiyama, Higashi-hiroshima 739-8526, Japan

dai-akase@hiroshima-u.ac.jp

Cyclodextrin (CD), a cyclic oligosaccharide of α-D-glucose, is one of the most important host molecules because of its ability to form inclusion complexes with various organic and inorganic guest molecules. The most common CD molecules are α-, β-, and γ-CDs containing six, seven, and eight glucopyranose residues, respectively (Figure 1). These molecules have the doughnut-like architecture with hydrophilic hydroxyl groups and a rather hydrophobic cavity. There are a primary and two socondary hydroxyl groups per residue, resulting in many conformers, and intermolecular and intermolecular hydrogen bonds. The solvation of CD molecules play a critical role in the inclusion process in aqueous solution, where CD molecules are partly desolvated upon forming inclusion complexes with guest molecules. In this study, we theoretically investigate α-, β-, and γ-CD molecules from the gas phase to aqueous solution in order to gain insight into intrinsic properties of CD molecules related to inclusion phenomena.

We performed geometry optimizations of various conformers of α-, β-, and γ-CD monomers and dimers at the B3LYP, ωB97X-D, and MP2 levels of theory with 6-31G(d,p) basis set. The DFT calculations were carried out using Gaussian09 program package and the MP2 calculations were carried out using NWChem program package. We also performed molecular dynamics (MD) simulations of aqueous CD solution using NAMD software package with CHARMM force field parameters. MD simulations were carried out for systems comprising a CD molecule and 5000 water molecules.

The results of gas phase quantum chemical calculations show that the lowest energy (including zero-point energy) conformers of α-, β-, and γ-CD monomer form homodromic hydrogen bonding network between primary hydroxyl groups. Three types of CD dimers, head-to-head, head-to-tail, and tail-to-tail dimers, are optimized. The binding energies of head-to-head and head-to-tail dimers are larger than that of tail-to-tail dimer. From the results of MD simulation, it is found that the homodromic hydrogen bonding network found in the gas phase calculation is broken and hydroxyl groups of CD molecules tend to hydrogen bond to water molecules. Water molecules are observed in the cavity of CD molecules and the number of water molecules in the cavity increase as the size of CD molecules. It is observed that one glucopyranose residue flips and occupies part of the cavity for α- and β-CD, whereas up to two glucopyranose residues flip for γ-CD. The flip of glucopyranose residues dramatically changes the solvation structure of CD molecules.

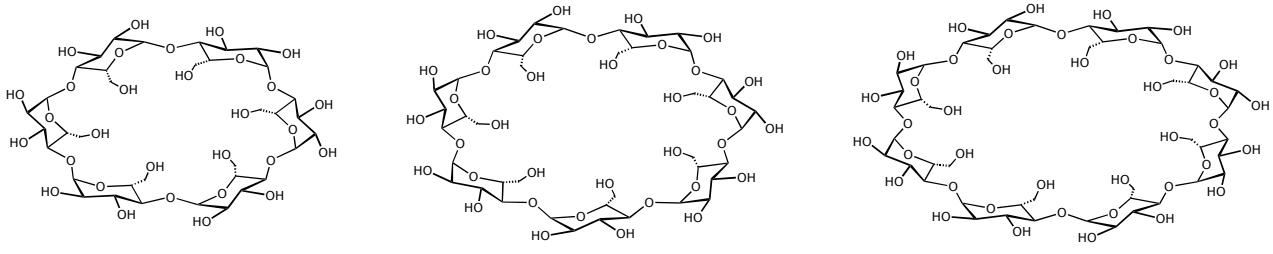

α-CD β-CD γ-CD

Figure 1. Chemical structures of cyclodextrin molecules.

PIb-03

Hydration Helmholtz energy of adamantane and halo-substituted adamantanes

Hideo Doi, and Misako Aida

Center for Quantum Life Science and Department of Chemistry, Graduate School of Science, Hiroshima University, 1-3-1 Kagamiyama, Higashi-hiroshima 739-8526, Japan

hideo-doi@hiroshima-u.ac.jp

I. Introduction

Adamantane ($C_{10}H_{16}$) is a highly symmetric tricyclic aliphatic hydrocarbon that is the simplest of the diamondoids. Adamantane is known as a valuable building block for polymers for the enhancement of their thermal stability or the improvement of their physical properties.

We focus on the hydration structures of adamantane and halo-substituted (fluorine or chlorine) adamantanes. We reveal how different the hydration structures of substituted adamantanes are.

II. Method

Geometry optimizations of various adamantantyl chloride or adamantly fluoride molecules were performed with MP2/aug-cc-pVDZ using the Gaussian09 program package. The natural population analysis (NPA) was used to calculate the atomic charges of the adamantane derivatives. The NPA charges were used to perform Monte Carlo (MC) simulations and free energy perturbation (FEP) calculation of aqueous adamantane derivatives together with the Lennard-Jones parameters [1] and TIP3P water model. MC simulations were carried out for the systems comprising an adamantane derivative molecule surrounded by 500 water molecules. The radius of a solvation sphere is set to be 15.4 Å, such that the density of adamantane molecule with 500 water molecules is 1 g cm^{-3}. The temperature of the system is set at 300K.

III. Results and Discussion

We dealt with 16 kinds of chlorine-substituted adamantanes, and 16 for fluorine-substituted adamantanes. The hydration helmholtz energy difference ΔA between adamantane and 1,3,5,7-tetrachloroadamantane was calculated to be +5.2 kcal/mol; i.e., the hydration helmhlotz energy of adamantane is lower than that is 1,3,5,7-tetrachloroadamantane. This indicates that chlorine atoms make adamantane more hydrophobic. The hydration helmholtz energy difference ΔA between adamantane and 1,3,5,7-tetrafluoroadamantane was −8.0 kcal/mol; i.e., the hydration helmhlotz energy of adamantane is higher than that of 1,3,5,7-tetrafluoroadamantane. This indicates that fluorine atoms make adamantane more hydrophilic. The substitution effects of fluorine and chlorine atoms on adamantane skeleton are opposite in the hydration helmhlotz energy.

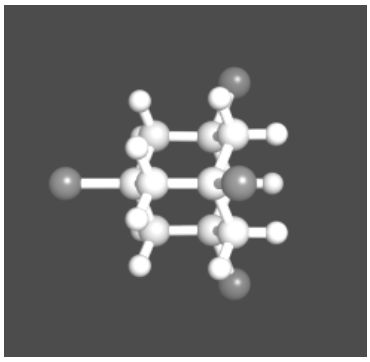

Fig. 1. 1,3,5,7-tetrachloroadamantane

[1] Freindorf M, Gao J., *J Comput. Chem.*, 17(3), 386–395 (1996).

PIb-04

Molecular Dynamics Simulation of the Photodesorption of Crystalline and Amorphous CO Ice in Interstellar Space

Marc C. van Hemert,[1] Junko Takahashi,[2] Ewine F. van Dishoeck[3]
[1]*Institute of Chemistry, University of Leiden, The Netherlands*
[2]*Meiji Gakuin University, Kamikurata-cho 1518, Totsuka-ku, Yokohama 244-8539, Japan*
[3]*Leiden Observatory, University of Leiden, The Netherlands*
e-mail address: juntaka@law.meijigakuin.ac.jp

I. Introduction

At the densities and temperatures in star-forming regions, all molecules other than H_2 should be kept frozen on dust grains within the timescales shorter than the interstellar cloud lifetimes. But, gaseous CO is detected there. Thermal desorption is negligible and thus photodesorption has been suggested as a possible mechanism. In the laboratory, this process has been simulated by depositing CO on a 10 K surface and following CO desorption upon irradiation of a D_2 discharge lamp [1,2]. In order to study this process theoretically, we performed classical molecular dynamics simulations of the CO molecule excited by a photon in the surface layers of crystalline-like and amorphous CO crystals at 10 K.

II. Method

For the ground state interaction potential of the CO-CO dimer, we performed ab initio CCSD calculations on a large grid of orientations and inter- and intra- molecular distances. We fit about 15000 data points to the interaction energy formula including the repulsive potential with the nonlinear alpha parameters, the dispersion potential, and the electrostatic potential. For the excited state, we used the contracted CI method where the two CO molecules lie in the same plane. We fit these data to the formula similar to the one used for the ground state, although we excluded all OCCO geometries.

We created crystalline-like and amorphous CO crystals consisting of 221-1055 and 200-1200 CO molecules, respectively. These crystals were modified by the molecular dynamics procedure of temperature cycling with the steps from 0 to 50 K and back to 10 K for 10000 cycles with 20 au (~0.5 fs) time step. Then, we brought a selected flake of the CO crystal into the excited state adiabatically with a photon of 8.7-9.9 eV. After the dynamics for 5000-10000 cycles with 4 au (~0.1 fs) time step, we brought back the flake into the ground state adiabatically and monitored the positions of CO molecules for another 50000 au.

III. Results and discussion

We found that there are two photodesorption mechanisms; (i) the direct mechanism where the excited CO molecule itself is released, and (ii) the indirect one where the excited CO molecule stays in the crystal but kicks out a neighboring molecule. Further, we found that the direct mechanism only occurs in the 1st surface shell and that the indirect one occurs in the 2nd surface shell. For the amorphous CO crystals, the direct and indirect photodesorption probabilities are 6-19 % and 4-16%, respectively. There are some effects of the photon energy and the size of crystals. For the crystalline-like CO crystals, only direct mechanism is observed and photodesorption probability is 2 %. Clearly the much more regular structure of crystalline-like crystals leads to stronger binding of surface molecules.

[1] Öberg et al., *Astrophys. J.*, **2007**, *662*, L23; *Astron & Astrophys.* **2009**. *496*, 281.
[2] Fayolle, E. C., et al., *Astrophys. J.*, **2011**, 739, L36.

PIb-05

Spontaneous Conformational Change of the C-terminal Region of U1A Suggests a Combined Mechanism of Conformational-selection and Induced-fit in the U1A-RNA Molecular Recognition

Ikuo Kurisaki[†,‡], Masayoshi Takayanagi[†,‡,§], *Masataka Nagaoka[†,‡]

[†]*Graduate School of Information Science, Nagoya University;* [‡]*CREST, JST;* [§]*Venture Business Laboratory, Nagoya University*

Graduate School of Information Science, Nagoya University, Furo-cho, Chikusa-ku, Nagoya 464-8601, Japan

e-mail address: kurisaki@ncube.human.nagoya-u.ac.jp

I. Introduction

The study of U1A-RNA complex formation mechanism has been a paradigm of protein-RNA molecular recognition. Tang and Nilsson discussed the induced-fit of U1A at the atomic level[1] (TN-conjecture), while Rupert et al. reported that an RNA accessible conformation appears under the presence of malonate acid (MLA) without the influence of RNA[2], suggesting conformational-selection of U1A's RNA recognition. It is, therefore, still controversial whether U1A recognizes RNA by induced-fit or conformational-selection.

II. Materials and Methods

We performed 25 molecular dynamics (MD) simulations of U1A both in the presence and absence of MLA. To characterize the conformations obtained from these simulations, root mean square deviation (RMSd), the residual solvent accessible surface area (SASA) and the interatomic distance were calculated.

III. Results and Discussion

To address this problem, we made such an assumption that *the reorientation of the C-terminal region does not necessarily occur "in response to the correct recognition of the RNA[1]" but under such an aqueous solution with MLA, or even without regard to the presence of MLA*. In fact, we found that U1A changed into the RNA-accessible conformation spontaneously, thus due to conformational-selection. However, the observed conformations were still incomplete with regard to stability and/or folded conformation. This indicates that "induced-fit" also works for the later process of complex formation. In conclusion, we propose that U1A-RNA molecular recognition is the combined mechanism of conformational-selection and "induced-fit". Finally, according to the observation, we propose a modification of the conventional conjecture of the U1A-RNA molecular recognition[3].

[1] Tang Y. and Nilsson L., *Biopyhys*. J., **77** (1999); [2] Rupert P.B. et al., *Acta Crystallo. Sect. D-Biol. Crystallo.* **59** (2004); [3] Kurisaki, I., Takayanagi, M. and Nagaoka, M. to be submitted.

PIb-06

Role of acidic proton in the decomposition of NO over dimeric Cu(I) active sites in Cu-ZSM-5 catalyst

P. K. Sajith, Yoshihito Shiota and Kazunari Yoshizawa*

Institute for Materials Chemistry and Engineering and International Research Center for Molecular Systems, Kyushu University, Fukuoka 819-0395, Japan

kazunari@ms.ifoc.kyushu-u.ac.jp (K.Y.)

The influence of proton in the mechanism of the direct decomposition of NO over adjacent dimeric Cu(I) active sites in zeolite was theoretically investigated with ONIOM (QM/MM) calculations. As previously proposed, the reaction proceeds through the formation of N_2O as a reaction intermediate and further its decomposition into oxygen and nitrogen. The present study showed that the presence of proton plays an important role in the production of N_2O from two NO molecules. This is due to the strengthening of the N–N bond by the proton attached to NO dimer, which facilitates the formation of N_2O. On the other hand, the presence of proton disfavors the decomposition of N_2O. The stable intermediate ZCu–OH^+–ZCu (where Z is an aluminum substitution site of the zeolite frame work) formed in the proton-assisted mechanism is responsible for the larger activation energy for N_2O decomposition. The proton-assisted NO decomposition mechanism is in agreement with the experimental observation that the decomposition of N_2O as well as O_2 desorption are the governing reaction steps in the decomposition of NO. The results disclosed herein will pave a way to understand the mechanism of the reductive N–N coupling of NO molecules catalyzed by metalloenzymes and transition metals.

PIb-07

A Study of Microrheology by the Time Dependent Density Functional Theory

Masao Inoue and Akira Yoshimori

Department of Physics, Kyushu University, Fukuoka 812-8581, Japan
e-mail address: m.inoue@cmt.phys.kyushu-u.ac.jp

Recently, mechanical properties of a complex fluid (i.e. a colloidal suspension, a polymer solution, etc.) have often been studied by observing motions of probe particles embedded into the fluid (microrheology). The motions depend on a density distribution of particles constituting the complex fluid around the probe particles. The density distribution is governed by interactions between constituting particles. Our purpose is to clarify effects of interactions between constituting particles on microrheology.

We consider a hard-sphere probe particle fixed at the origin and colloidal particles suspended in a solvent, which flows at a velocity **U**. In this system, the probe particle is subjected to the force **F** exerted by colloidal particles. Then, we calculate **F** by considering two cases of interactions between colloidal particles: hard-sphere interactions and no interactions. In the present study, we focus on **F** for small volume fractions of colloidal particles.

To this system, we apply the time dependent density functional theory (TDDFT). The theory has been successful in describing the dynamics of molecular liquids [1] and colloidal dispersion systems. By calculating the TDDFT numerically, we obtain the force **F** from the density distribution of colloidal particles around the probe particle.

Calculated results show that the force acting on the probe particle decreases because of hard-sphere interactions between colloidal particles. The force **F** obtained with hard-sphere interactions (symbols in Figure) is smaller than that obtained without interactions (solid line in Figure). A significant effect of the interactions is caused by increase in a volume fraction of colloidal particles ϕ or decrease in a size of a colloidal particle b. In addition, the effect becomes weak as the velocity **U** becomes fast.

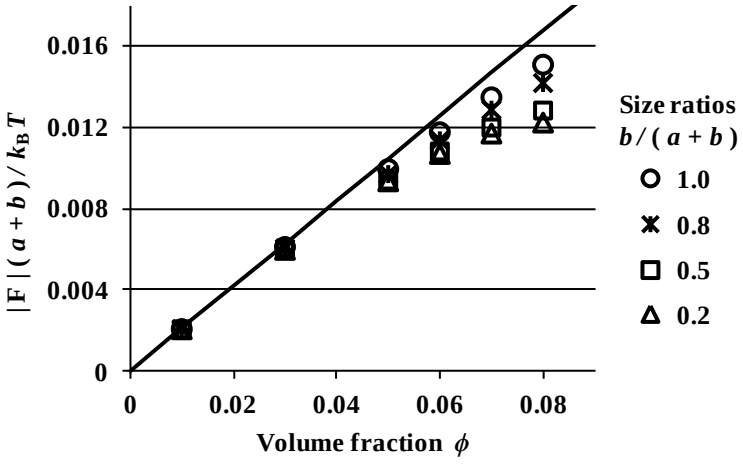

Figure: Volume fraction dependence of the force **F**. Symbols represent results obtained with hard-sphere interactions between colloidal particles. A solid line represents results obtained without interactions. Here, a and b are radii of a probe and a colloidal particle. The velocity **U** is given by $(a+b)|\mathbf{U}|/D = 0.1$, where D is a diffusion coefficient of the colloidal particles.

[1] A. Yoshimori, J. Theor. Comput. Chem. **03** (2004) 117

PIb-08

Explicit solvent effects on vibrational spectra of glycine: Vibrational frequency analysis using analytical Hessian

Yukichi Kitamura[1,2], Norio Takenaka[1,3], Yoshiyuki Koyano[1], and Masataka Nagaoka[1,3]

[1] *Graduate School of Information Science, Nagoya University, Nagoya 464-8601, Japan*

[2] *Research Fellow of Japan Society for the Promotion of Science (JSPS), Tokyo 102-0083, Japan*

[3] *ESICB, Kyoto University, Katsura, Kyoto 615-8520, Japan*

e-mail address: y-kitamura@ncube.human.nagoya-u.ac.jp

I. Introduction In gas phase, to identify equilibrium structures, interpreting their molecular characteristics, the vibrational frequency analysis (VFA) has been quantum-chemically achieved and has been successfully used. On the other hand, in solution, it is common to employ additionally the dielectric continuum approximation although some serious problems were reported [1]. Hence, we have developed the VFA in solution using the analytical Hessian averaged over the equilibrium QM/MM-MD trajectory [2]. Then, we have applied it to neutral-form glycine in aqueous solution, and discussed the microscopic solvation effects [1,2].

II. Method We have first obtained the equilibrium structure in solution by the free energy gradient (FEG) method [3]. Then, the effective vibrational frequencies in solution were estimated by diagonalizing the free energy Hessian matrix (in Eq. 1) [2,3]. The AMBER-GAUSSIAN interface (AG-IF) [4] was used to execute the QM/MM-MD simulation.

$$\left\langle \frac{\partial^2 V_{\mathrm{SB}}\left(\mathbf{q}^{\mathrm{S}}\right)}{\partial \mathbf{q}_a^{\mathrm{S}} \partial \mathbf{q}_b^{\mathrm{S}}} \right\rangle_{\mathbf{q}^{\mathrm{B}}} = \left\langle \frac{\partial^2 \left\langle \Psi \middle| \hat{H}_{\mathrm{QM}} + \hat{H}_{\mathrm{QM/MM}}^{\mathrm{est}} \middle| \Psi \right\rangle}{\partial \mathbf{q}_a^{\mathrm{S}} \partial \mathbf{q}_b^{\mathrm{S}}} \right\rangle_{\mathbf{q}^{\mathrm{B}}} + \left\langle \frac{\partial^2 \hat{H}_{\mathrm{QM/MM}}^{\mathrm{vdW}}}{\partial \mathbf{q}_a^{\mathrm{S}} \partial \mathbf{q}_b^{\mathrm{S}}} \right\rangle_{\mathbf{q}^{\mathrm{B}}} \qquad (1)$$

III. Results and discussion **Fig. 1** shows the IR spectra in the high-frequency region in gas phase and solution. As for stretching modes of OH and NH_2 groups, the vibrational frequencies are red-shifted by the environmental change from gas phase to solution. On the other hand, those for bending modes are blue-shifted in general. Our results are in good agreement with the experimental ones [5]. Furthermore, to clarify the microscopic origin of such vibrational shifts, we have examined the structural relaxation of equilibrium structure and the solvation structure. As a result, it was found that the H-bonding formation brings about weakening of the stretching motion due to the bond length elongation. On the other hand, blue shifts of bending modes are attributed to the hindrance of the motion by adjacent solvent water molecules.

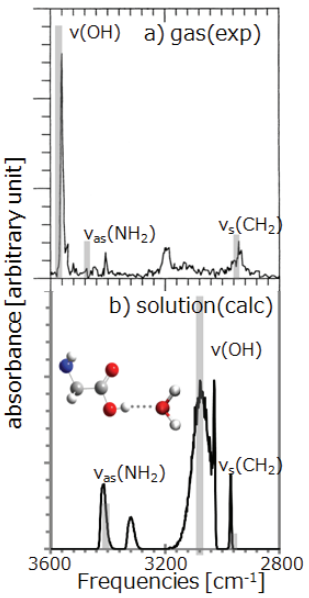

Fig. 1. Frequency shifts in high-frequency regions.

[1] (a) Y. Kitamura, et al., *Chem. Phys. Lett.*, **514**, 261 (2011); (b) O. Acevedo, et al., *J. Am. Chem. Soc.*, **128**, 6141 (2006). [2] Y. Kitamura, et al., in preparation. [3] (a) M. Nagaoka, et al., *J. Phys. Chem. A.*, **102**, 8202 (1998); (b) N.Okuyama-Yoshida, et al., *Int. J. Quantum Chem.*, **70**, 95 (1998). [4] T. Okamoto, et al., *J. Comp. Chem.*, **32**, 932 (2011). [5] B. Boeckx, et al., *J. Phys. Chem. B.*, **116**, 11890 (2012).

PIb-09

A new theoretical approach to find single bond activation pathways on metal cluster: A case study of H_2 dissociation on gold clusters

Min Gao, Satoshi Maeda, Andrey Lyalin, and Tetsuya Taketsugu
Department of Chemistry, Faculty of Science, Hokkaido University, Sapporo, 060-0810, Japan
E-mail address: gaomin@mail.sci.hokudai.ac.jp

Metal clusters have attracted great interest due to their wide applications in the areas of biology, catalysis, and nanotechnology. Single bond activation, such as, O-O, H-H bond etc., is one of the most studied cases to investigate the catalytic activity of metal clusters. To predict the most favorable pathway for single bond activation, it is important to compare all the reaction pathways with low reaction barriers. However, it is a very hard task to find all low-lying pathways even for simple single bond activation. It is necessary to consider activation pathways on several low-lying isomers including the most stable one, since there is experimental evidence that several metal isomers can coexist at mild temperature [1]. To our best knowledge, there is no systematic and effective way to get all the possible pathways for single bond activation catalyzed by several low-lying isomers of metal cluster.

In the present study, a new approach is proposed to find automatically single bond activation pathways on metal clusters with using a combination of anharmonic downward distortion following (ADDF) method and artificial force induced reaction (AFIR) method. We applied the approach to H_2 dissociation reactions on small gold clusters. Many equilibrium structures of gold clusters and H_2 dissociation pathways with low energy barrier were obtained. It was shown that the less stable isomer of gold cluster is also catalytically active for H_2 dissociation (Fig.1). The present strategy automatically identified the lowest energy TS for H-H bond activation efficiently with a systematic procedure.

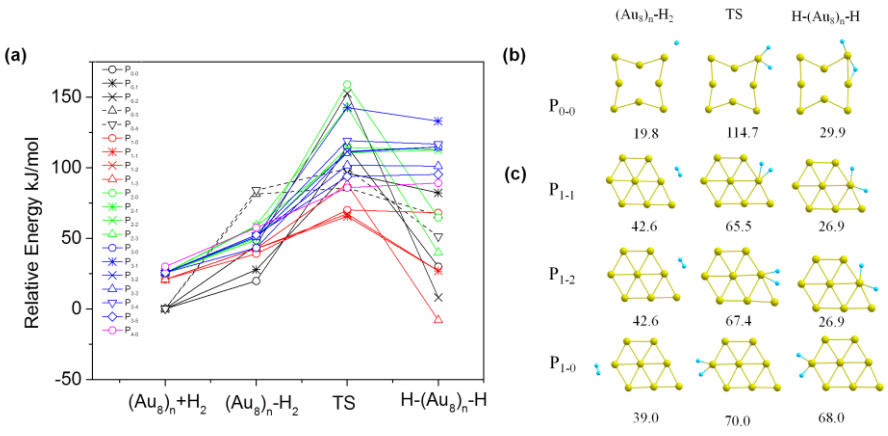

Fig.1 (a) Potential energy profiles for H_2 dissociation on isomers of Au_8. (b) Structures along the pathway starting from the most favorable adsorption geometry. (c)Structures along the three lowest pathways.

[1] Gruene, P.; Rayner, D.M.; Redlich, B.; Meijer, G.; *et al*., Fielicke, A., *Science* **2008,** 321, 674-676.

PIb-10

Methane C–H bond Activation by Iron-Oxo Embedded Graphene: A Density Functional Theory Approach

Sarawoot Impeng[1,2], Chompunuch Warakulwit[1,2], Pipat Khongpracha[1,2], Jumras Limtrakul[1,2] and Masahiro Ehara[3]

[1]*Department of Chemistry, and NANOTEC Center for Nanoscale Materials Design for Green Nanotechnology, Kasetsart University, Bangkok 10900, Thailand*

[2]*Center for Advanced Studies in Nanotechnology and Its Applications in Chemical, Food and Agricultural Industries, Kasetsart University, Bangkok 10900, Thailand*

[3]*Institute for Molecular Science and Research Center for Computational Science, 38 Nishigo-naka, Myodaiji, Okazaki 444-8585, Japan*

e-mail address: ehara@ims.ac.jp

I. Introduction

Methane C–H bond activation and its subsequent oxidation into value-added chemical at room temperature has received much attention because it is not only challenging but also there is a high demand for catalysis [1]. It has been found that the metal-oxo catalyst especially iron-oxo can accomplish such reaction; for example, those in enzyme or zeolite systems [1]. Herein, we have studied the C–H bond activation of methane over iron-oxo embedded graphene (O–Fe-Graphene) by using the density functional theory (DFT) calculations.

II. Methodology

In this work, the periodic DFT calculations were performed at the PBE/DNP level of theory. In order to obtain more reliable energetics, the single point energy calculations with dispersion corrected functional were carried out.

III. Results and Discussion

Two possible spin states, namely, singlet and triplet states, were examined for methane activation. It was found that the triplet state is kinetically preferred than singlet state (17.4 *vs* 31.0 kcal/mol) while it is not thermodynamically stable (12.8 *vs* –7.7 kcal/mol) in the reaction pathway (see Fig. 1). From this result, it can be deduced that both spin states play a vital role for methane activation similar to the previous work [2]. The detail of the reaction mechanism, relative energies and all optimized structures along the reaction pathways will be discussed in the presentation.

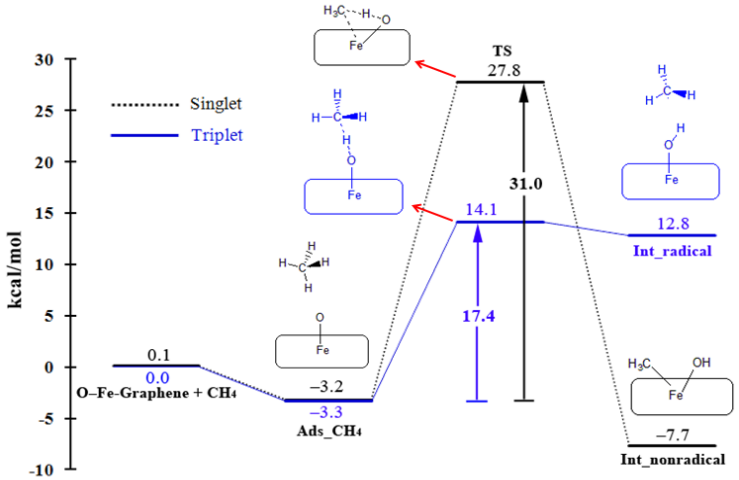

Fig. 1. Energy profile for methane activation over O–Fe-Graphene.

[1] Hammond, C.; Conrad, S.; Hermans, I. *ChemSusChem* **2012,** *5*, 1668–1686.
[2] Schröder, D.; Shaik, S.; Schwarz, H. *Acc. Chem. Res.* **2000,** *33*, 139–145.

PIb-11

Impact of intermolecular interaction on the second hyperpolarizability of phenalenyl radical dimer

Kyohei Yoneda, Kotaro Fukuda, Hiroshi Matsui, Yuta Hirosaki, Shota Takamuku, and Masayoshi Nakano

Department of Materials Engineering Science, Graduate School of Engineering Science, Osaka University, Toyonaka, Osaka 560-8531, Japan

e-mail address: yoneda@cheng.es.osaka-u.ac.jp

I. Introduction

In previous studies, we have theoretically found that the second hyerpolarizability (γ) [the microscopic origin of the third-order nonlinear optical (NLO) property] for open-shell singlet systems shows a strong diradical character *y* dependence: the systems having intermediate diradical characters tend to exhibit a large enhancement of γ as compared to the closed-shell (*y* = 0) and pure diradical systems (*y* = 1) [1]. Furthermore, it has been clarified that for a realistic dimer composed of diphenalenyl diradicaloids, the dimerization enhances the γ value per monomer as compared with that of the isolated monomer, which is caused by the emergence of a tetraradical nature due to the covalent-like intermolecular interaction through their radical sites [2]. This result indicates the significant impact of the intermolecular interaction in the open-shell dimers on the open-shell character. In this study, in order to elucidate the fundamental relationships between the intermolecular interaction, diradical character and NLO property, we investigate the π-π stacked phenalenyl radical dimers, which are predicted to exhibit singlet diradical ground states, with different intermolecular distances.

II. Results and Discussion

Fig. 1 shows the stacking distance (*d*) dependence of the *y* and γ per monomer (= γ/2) for the phenalenyl dimers calculated by the LC-UBLYP/6-31G* method. It is found that the systems show a wide range of *y* values depending on the stacking distances and that the variation strongly affects their γ values: the γ per monomer for the system with intermediate diradical character (*y* = 0.299, γ/2 = 9.30×10^4 a.u. at *d* = 3.0Å) is about 30 times enhanced as compared to that of the isolated phenalenyl monomer (γ = 2.98×10^3 a.u.). Details as well as the results of tetramers are presented in the poster session.

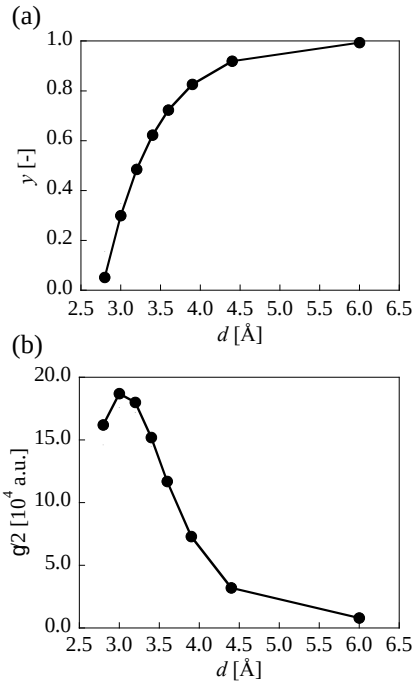

Fig. 1. Stacking distance (*d*) dependence of *y* (a) and γ/2 (b) values for the phenalenyl dimers

References

[1] M. Nakano, et al., *J. Phys. Chem. A* **109**, 885 (2005); *Phys. Rev. Lett.* **99**, 033001 (2007).
[2] M. Nakano et al., *Chem. Phys. Lett.* **454**, 97 (2008).

PIb-12

Systematic exploration of reaction mechanisms for a vinylogous Mannich-type reaction activated by a water molecule: kinetic control vs. thermodynamic control

Ryohei Uematsu, Satoshi Maeda, and Tetsuya Taketsugu
Graduate School of Chemical Sciences and Engineering, Hokkaido University, N10-W8, kita-ku, Sapporo 060-0810, Japan
e-mail address: ryohei_uematsu@mail.sci.hokudai.ac.jp

I. Introduction

The five-substituted γ-butenolide motif and its derivatives, which are seen in a munber of natural products, are useful building blocks of various compounds. Recently, Landelle et al. reported the efficient synthesis of δ-amino-γ-butenolide in good yield by only mixing an amine, an aldehyde, and 2-trimethylsiloxyfuran (TMSOF) at room temperature under solvent free conditions [1] as shown in Scheme 1.

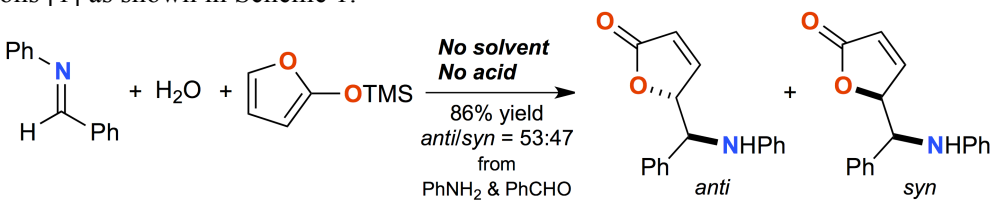

Scheme 1. Vinylogous Mannich-type reaction using TMSOF

However, unlike typical Mannich reactions, the mechanism of the present reaction, which proceeds under nonacidic conditions without catalyst, was not well understood. Hence, we studied the mechanism using the artificial force induced reaction (AFIR) method [2].

II. Results and Discussion

The AFIR method identified as many as five working pathways [3]. The main pathways in this reaction are shown in Fig. 1. Among them, two concertedly produce *anti*- and *syn*-isomers of the product. The other two once give an intermediate, a regioisomer of the main product. This intermediate can be consumed rapidly through retro-Mannich reaction giving a pair of intermediates, imine and 2-furanol. The remaining path directly generates this intermediate pair. These imine and 2-furanol easily react to each other affording the product. These intermediates never gain sufficient population owing to the existence of faster channels than their generation. In other words, the final ratio of each species should be controlled by their thermodynamic stability as well as barrier heights for their generation.

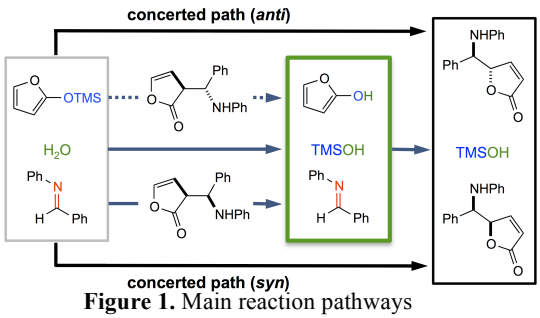

Figure 1. Main reaction pathways

[1] Landelle, G.; Claraz, A.; Oudeyer, S.; Levacher, V. *Tetrahedron Lett.* **2012**, *53*, 2414-2416.

[2] Maeda, S.; Ohno, K.; Morokuma, K. *Phys. Chem. Chem. Phys.* **2013**, *15*, 3683-3701.

[3] Uematsu, R.; Maeda, S.; Taketsugu, T. *Chem. Asian J.* **2013.** [DOI: 10.1002/asia.201301065].

PIb-13

Effects of the Silyl Substituent of Diphenylprolinol Silyl Ether in the Organocatalyst-Mediated Asymmetric Reactions: Computational and Experimental Investigations

Tadafumi Uchimaru,[1]* Seiji Tsuzuki,[1] Daichi Okamura,[2,3] Tatsuya Yamazaki,[3] Yasuto Ameda,[3] Hiroaki Gotoh,[3] Yujiro Hayashi[2,3]*

[1]*Nanosystem Research Institute, Advanced Industrial Science and Technology*

[2]*Department of Chemistry, Graduate School of Science, Tohoku University*

[3]*Department of Industrial Chemistry, Faculty of Engineering, Tokyo University of Science*

e-mail address: t-uchimaru@aist.go.jp, yhayashi@m.tohoku.ac.jp

Diarylprolinol silyl ether is one of the privileged organocatalysts, developed by our group [1] and Jørgensen's group [2] independently. It is an effective catalyst for asymmetric reactions involving reactive intermediates such as enamine and iminium ion. Recently Seebach and coworkers carried out X-ray crystallographic analysis of the iminium salts **3** and **4** generated from diphenylmethylsilylated and trimethylsilylated ethers **1** and **2** with cinnamaldehyde and also enamine **5** derived from **1** and phenylacetaldehyde [3]. Starting from the X-ray crystal structures, we performed conformational analysis of iminium ions **3**, **4** and the enamine **5** using CONFLEX 7 [4] with MMFF94s force field [5]. Furthermore, we carried out DFT calculations at the B3LYP/6-31G(d) and M06-2X/6-311+G(2df,2p) levels. The structures of the lowest energy conformers of the iminium ions **3**, **4** and the enamine **5**, are shown below. The top face of the pyrrolidine ring is covered with bulky substituent $–CPh_2(OSiMe_3)$/$–CPh_2(OSiPh_2Me)$. Consequently, the top face approach of a reagent to iminium ions **3** and **4** and also top face approach of a reagent to enamine **5** will be energetically disfavored as compared to the bottom face approach. This is a main reason for the enantiomeric differentiation of diphenylmethylsilylated and trimethylsilylated ether catalysts **1** and **2**. Furthermore, the silyl substituent effect on the enantioselectivity according to the reaction types and the difference in reactivity between catalysts **1** and **2** are reasonably explained based on the conformational analysis of iminium ions and enamine via theoretical calculations. These points and also the differences between the solid structures and calculated structures will be presented and discussed in detail.

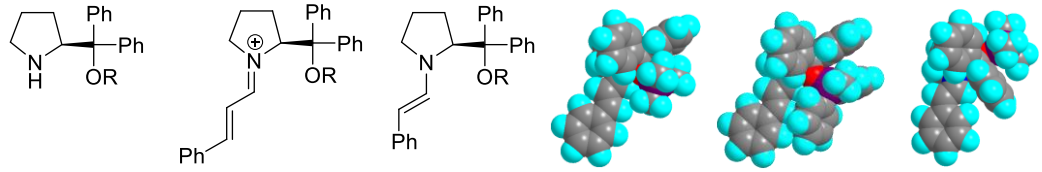

1: R = $-SiMe_3$ **2**: R = $-SiPh_2Me$ **3**: R = $-SiMe_3$ **4**: R = $-SiPh_2Me$ **5**: R = $-SiMe_3$

Figure. Left) Chemical structures of diphenyl prolinol silyl ether catalysts **1** and **2**, iminium intermediate **3** and **4**, and enamine intermediate **5**. (Right) the lowest energy conformers of the iminium ions **3**, **4** and the enamine **5**

[1] Y. Hayashi et al. *Angew. Chem. Int. Ed.* **2005**, *44,* 4212. [2] K. A. Jørgensen et al. *Angew. Chem. Int. Ed.* **2005**, *44,* 794. [3] (a) D. Seebach et al. *Helv. Chim. Acta* **2008**, *91,* 1999. (b) D. Seebach et al. *Helv. Chim. Acta* **2009**, *92,* 1225. [4] CONFLEX 7, H. Goto et al. CONFLEX Corporation, Tokyo, Japan, 2012. [5] (a) T. A. Halgren, *J. Comput. Chem.* **1999**, *20,* 720. (b) T. A. Halgren, *J. Comput. Chem.* **1999**, *20,* 730.

PIb-14

Diradical character based design for singlet fission in heteroacene molecules

Soichi Ito and Masayoshi Nakano

Department of Materials Engineering Science, Graduate School of Engineering Science, Osaka University, Toyonaka, Osaka 560-8531, Japan
e-mail address: soichi@cheng.es.osaka-u.ac.jp

Singlet fission is one of the multiple exiton generation processes in which singlet exciton splits into two triplet excitons, and it has been shown that singlet fission can increase the energy conversion efficiency of a photovoltaic cell. In order to achieve exoergic or isoergic fission, $2E(\mathrm{T}) - E(\mathrm{S}) \leq 0$ [condition (i)] should be satisfied [1], where $E(\mathrm{S})$ and $E(\mathrm{T})$ is the lowest singlet and triplet excitation energy, respectively. In addition, $E(\mathrm{T})$ must be high enough to carry sufficiently large energy and to have large driving force for charge separation event at the donor/acceptor interface. Our previous study [2] has shown that a molecule with weak/intermediate diradical character y_0 is favorable to satisfying (i), where y_0 is an index of the instability of a chemical bond and is defined by the occupation number of the lowest unoccupied natural orbital. Since molecules shown in Scheme 1 have both zwitterionic and diradical resonance structures, they are expected to have non-negligible diradical character y_0 and to be good candidates for satisfying condition (i). The restricted active space second order perturbation theory (RASPT2) method reveled that two weak/intermediate diradical molecules, **N0-3** and **N2-4**, are promising candidates for efficient singlet fission (Table 1) that satisfy (i) with relatively high $E(\mathrm{T})$. These results agree with our previous study [2]. The details of the relationship between diradical character and molecular structure will be presented in the poster session.

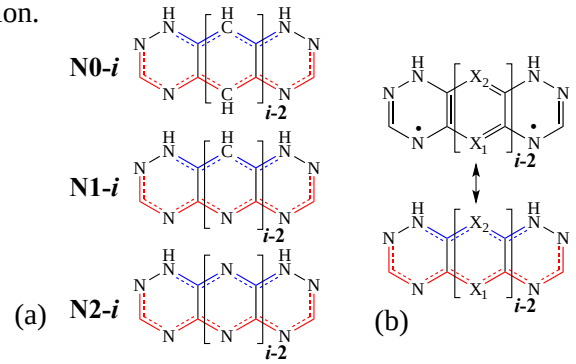

Scheme 1. Molecular structures of **N0-*i***, **N1-*i*** and **N2-*i***, where **N*m*-*i*** represents ***m*** nitrogen atoms per one central six-membered rings and ***i*** is the number of the central rings (a), and diradical and zwitterionic resonance structures of the molecules (X_1, X_2 = CH or N) (b).

Molecule	y	E(S)	E(T)
N0-3	0.32	2.41	1.10
N1-3	0.19	2.57	1.36
N2-3	0.15	2.71	1.56
N0-4	0.63	1.75	0.48
N1-4	0.53	2.13	0.80
N2-4	0.27	2.60	1.08

Table 1. Diradical character y_0, excitation energies of lowest singlet [E(S)] and triplet [E(T)] states.

[1] M. B. Smith and J. Michl *J. Chem. Rev.* **2010**, *110*, 6891.
[2] T. Minami and M. Nakano, *J. Phys. Chem. Lett.* **2012**, *3*, 145; T. Minami, S. Ito and M. Nakano, *J. Phys. Chem. Lett.* **2012**, *3*, 2719; *J. Phys. Chem. Lett.* **2013**, *4*, 2133.

PIb-15

Theoretical evaluation of photostability for Sun Protect molecule in UV energy region

(Sophia University[1] , Individual[2]) Ryota Shimada[1] , Toshimasa Ishida[2] , Shinkoh Nanbu[1]
E-mail : ry-shima@hoffman.cc.sophia.ac.jp

We investigated relaxation mechanism of sun screen molecules after photoexcitation by theoretical method based on ab-initio calculation .

The molecules are Alkyl Metohxy Cinnamate (AMC) groups, and have absorption area in UV region (UVA ; 400～315 nm, UVB ; 315～280 nm, UVC ; 280～10 nm). After photoexcitation, the molecules move back toward the ground state through non-adiabatic process. During the process, the molecules aren't destroyed and don't generate unhealthy side product. So these molecules are used as drug to protect human skin from UV.

The non-adiabatic transition are caused by geometric change of the molecules and especially *cis-trans* reciprocal change have dominant role of the non-adiabatic transition. Though these are not enough exposition, several previous works(*) in experimental area has reported the *cis-trans* reciprocal change of AMC molecules. We think detailed understanding of *cis-trans* reciprocal change of the molecules is very important basis for development of better Sun Screen molecules.

We researched several AMC molecules in this work. To clarify the non-adiabatic process of the molecules after photoexcitation. We performed non-adiabatic MD simulation by Trajectory Surface hopping (TSH) method based on Zhu-Nakamura theory.

Methyl Metoxy Cinnamate (MMC) is one of molecules which we have researched. This molecule is the smallest AMC molecules. We applied TSH method to both *cis* form and *trans* form of this molecule. In the both form, geometric parameter which caused non adiabatic transition is *cis-trans* reciprocal change. But *cis* form and *trans* form shwed different *cis-trans* reciprocal change type respectively.

We also researched bigger AMC molecule compare to MMC molecule and performed same calculation to understand alkyl size dependence of the non-adiabatic process of AMC molecules . And we compared these results to the result of MMC molecule.

In the poster session, we will present more detail discussion.

(*)M.M Jiménez , *International Journal of Pharmaceutics* , **272** , 1–2 ,19 March 2004 , 45-55

PIb-16

Ground state study of LiX, NaX, KX and RbX (X = Ca, Sr) polar molecules

Geetha Gopakumar[1,2], Minori Abe[1,2], Masahiko Hada[1,2] and Masatoshi Kajita[3]

[1]*Department of Chemistry, Tokyo Metropolitan University, 1-1 Minami-Osawa, Hachioji Tokyo, 192-0397, Japan,*

[2]*JST, CREST, 4-1-8 Honcho, Kawaguchi, Saitama, 332-0012, Japan*

[3]*National Institute of Information and Communications Technology, Koganei, Tokyo 184-8795, Japan*

e-mail address: geetha@tmu.ac.jp

Creation of ground-state polar molecules in the sub-micro kelvin regime is one of the most important achievements in atomic, molecular and optical physics in recent years. Such "ultracold" samples have found many exciting applications. Some notable applications of ultracold high-precision measurements are the search of electron electric dipole moment (eEDM)[1] by charge-parity (CP) violation and test of the variance in the proton-to-electron mass ratio (m_p/m_e)[2]. To understand the feasibility of manipulating ultracold polar molecules for such study, first hand information of ground state energy structure and permanent dipole moment (PDM) are invincible.

In this poster, we investigate the electronic ground state properties of XLi, XNa, XK and XRb (X =Ca, Sr) ultracold polar molecules. We obtain potential energy curves (PEC) (Fig. 1(a)) at the coupled cluster singles and doubles with partial triples [CCSD(T)] level of electron correlation. Further starting from CCSD(T) PECs, permanent dipole moments (PDM) (Fig. 1(b)) and static dipole polarizabilities (Fig. 1(c)) are obtained by finite field perturbation theory (FFPT). We report spectroscopic parameters; equilibrium bond length R_e, dissociation energy D_e, harmonic constant ω_0, number of bound states, N_v, rotational constant B_0, permanent dipole moment d_0, average polarizability α_0, polarizability anisotropy $\Delta\alpha_0$ and C_6 coefficient for the intermolecular dispersion interaction between molecules in the ground $v = 0$, $J = 0$ vibrational level. Ro-vibrational information of the lowest $v = 0$, $J = 0$ can further be used for the understanding of stability of ultracold samples against collisions.

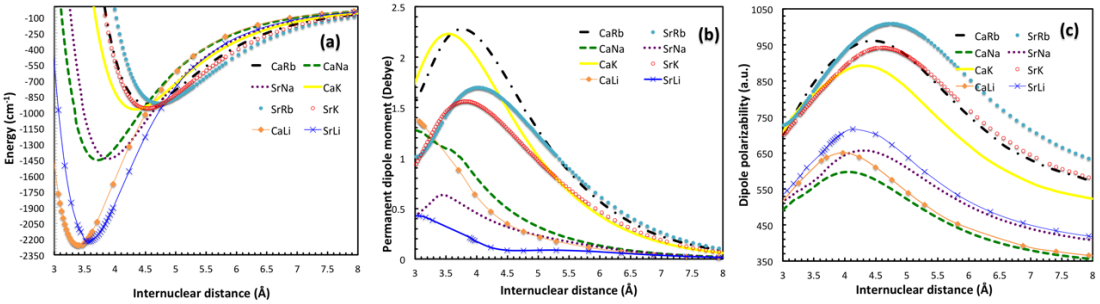

Fig.1 Potential energy curves (a), permanent dipole moments (b) and static dipole polarizabilities (α) of the electronic ground state of XLi, XNa, XK and XRb (X= Ca, Sr) molecules.

[1] Hudson et *al*, Nature 473, 493–496 (2011)

[2] M Kajita, G. Gopakumar, M Abe and M Hada, Lab talk, http://iopscience.iop.org/0953-4075/labtalk-article/52131 (2013)

PIb-17

A reparametrization approach of the B3LYP functional based on the equilibrium temperature of the spin crossover compounds.

Ahmed Slimani, Xuefang Yu, Koichi Yamashita

Department of Chemical System Engineering, The University of Tokyo 7-3-1, Hongo, Bunkyo-Ku, Tokyo 113-8656, Japan

e-mail address: ahmed@tcl.t.u-tokyo.ac.jp

The theoretical study of the electronic structure of spin-crossover compounds is very challenging due to the technical limitations of highly accurate ab initio methods and/or the inaccuracies of density functional methods in the prediction of low-spin/high-spin energy splitting. However, calculations using a reparametrized functionals could improve considerably the results. In this communication, we present an investigation of the HS/LS energy gap of $Fe(btr)_2(NCS)_2.H_2O$ spin crossover compound using several DFT functionals. The derived results exhibit a large deviation and several methods mis-estimate the HS/LS energy splitting. Such effect point out the need for a leader criterion resulting the usage of the suitable DFT functional and consequently a reasonable estimation of the HS/LS energy splitting. We propose a reparametrization approach of the B3LYP* functional based on the equilibrium temperature of the spin crossover compound. Such reparametrization leads to $19.8\,kJ/mol$ as HS/LS energy splitting comparable with the value calculated using DFT+U technique. In fact, such approach is very helpful to match the reparametrized B3LYP functional to the considered spin crossover compound. The resulting configuration coordinate diagram was as well investigated (see fig.1).

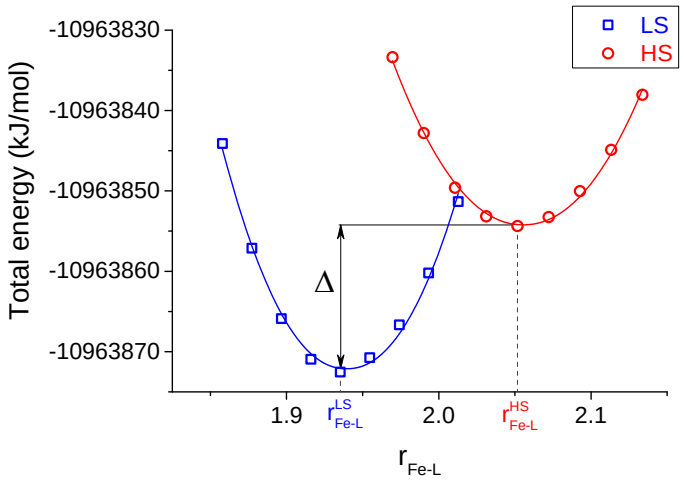

Figure 1: The configuration coordinate diagram computed with B3LYP (c=0.11) within 6-31G(d) basis set.*

PIb-18

Metal Dependency and Protein Environment Effect on the Optical and Electronic Properties of Metalloporphyrin-Ligand Systems

Mitsumasa Abe, Masami Lintuluoto
Graduate School of Life and Environmental Sciences, Kyoto Prefectural University, Shimogamo, Sakyo-ku, Kyoto 606-8522, Japan
e-mail address: masami@kpu.ac.jp

I. Introduction

Nitric oxide (NO) is involved in stress physiology and stress-related disease processes. The sensor to measure NO concentration in bodies is essential for interpretation of pathogenic mechanisms and predictions of paroxysmal attack. Hemoglobin (Hb) has been often used for the NO sensor development. However, the Hb-based NO sensors have problems including the denaturation of the protein moiety of Hb and the inconvenience of the operations. In this study, we investigated the details of metal dependency and the roles of amino acid residues surrounding heme on the NO coordination to metalloporphyrin by using three models (HEME, HB and M[OMP]).

II. Computational Methods

Ligands, such as NO and O_2 coordinate to the Fe atom of heme in Hb. We first investigated the NO coordination to iron porphyrin by using the model HEME and compared to the results of the O_2 coordination. Then, we studied the beta-globin of human Hb to investigate effect of protein environment around heme on the NO coordination to Hb by using the model HB. The model M[OMP] which is metal octamethylporphyrin, is used to investigate metal dependency on the NO coordination. QM/MM method was used to evaluate influence of protein environment. Protein in the MM region was replaced with point charge by using the AMBER 99 parameters. The QM region (metalloporphyrin) was calculated by using B3LYP with LANL2DZ basis set for metal atoms and 6-31G(d) basis set for H, C, N, and O. In addition, TDDFT calculation was carried out to obtain UV-vis absorption spectra.

III. Results and Discussion

The changes of HOMO and LUMO energy levels on the NO and O_2 coordination to heme center by using the model HEME were first studied (Table 1). The results of the model HB did not notably vary. Metal dependency and effect of protein on the changes of HOMO and LUMO energy levels will be discussed.

CIE *xy* chromaticity coordinates were next performed by using the results of TDDFT calculations. If chromaticities greatly change, it helps visualization of the NO coordination to metalloporphyrin. We will report the chromaticity on various models.

Table 1. HOMO and LUMO energy levels [a.u.]

	HEME	HEME-NO	HEME-O_2
HOMO	-0.19363	-0.19559	-0.19818
LUMO	-0.08918	-0.08975	-0.13563

PIb-19

Localized vs. Delocalized Ground and Excited states of Mn(III) and Ni(II) Salen Complexes: Theoretical Study of Solvation Effects

Shinji Aono, Masayuki Nakagaki, and Shigeyoshi Sakaki
Fukui Institute for Fundamental Chemistry, KyotoUnisversity,
34-4 Takano Nishihiraki-cho, Sakyo-ku, Kyoto 606-8103, Japan
e-mail address: saono@fukui.kyoto-u.ac.jp

One-electron-oxidized Mn(III) and Ni(II) salen complexes exhibit unique mixed valence electronic structure and charge transfer (CT) absorption. For instance, the one-electron oxidized Mn(III) salen complex shows the broad and weak absorption (class II mixed valence complex by Robin -Day classification) in solution but the one-electron oxidized Ni(II) salen complex shows the sharp and strong absorption (class III) when the salen ligand is symmetrical (R_1=R_2); see Scheme 1 for structures. The former absorption was experimentally discussed by the inter-valence CT (IVCT) from the phenolate anion to the phenoxyl radical moiety and the latter is the excitation from the doubly-occupied delocalized π_1 orbital to the singly-occupied delocalized π_2 orbital;[1] see Scheme 2. To elucidate these different features between the Mn(III) and Ni(II) complexes, the geometries of the complexes and the solvent distributions were optimized by the three dimensional reference interaction site model self-consistent field (3D-RISM-SCF) method.[2] The vertical excitation energy, ΔE, and the oscillator strength, *f*, were evaluated at the general multi-configuration reference quasi-degenerate perturbation theory (GMC-QDPT) level[3] by including the solvation effect based on the above optimized solvent distribution. The theoretical calculations provide a reasonable agreement with the experimentally observed absorption spectra and reproduce the differences between the Mn(III) and the Ni(II) and those among the salen ligands, as shown in Table 1. Solvation effect is indispensable for correctly describing the mixed-valence character, the geometrical distortion, the electronic localization, and the IVCT absorption of these complexes.

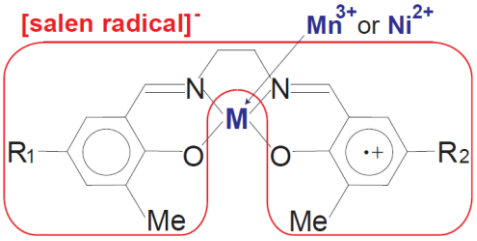

Scheme 1. Structure of metal-salen complex

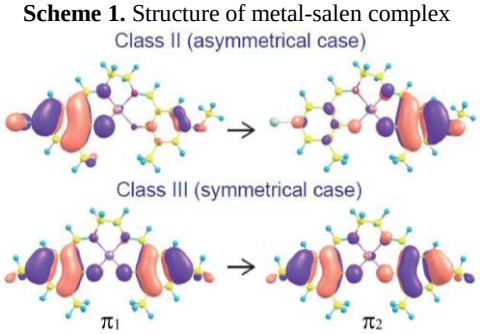

Scheme 2. Difference in absorption character

Table 1. Vertical excitation energy ΔE [eV] and oscillator strength *f* in CH_2Cl_2 solution

	Mn(III)			Ni(II)		
(R_1, R_2)	(Me, Me)	(OMe,OMe)	(OMe, Cl)	(Me, Me)	(OMe,OMe)	(OMe,Cl)
Calc. ΔE	1.126	1.208	1.839	0.449	0.437	1.423
Calc. *f*	0.081	0.124	0.061	0.375	0.377	0.119
Expt. ΔE	0.838	0.976	1.389	0.620	0.579	0.885

[1] T. Kurahashi and H. Fujii, *J. Am. Chem. Soc.* **2011**, 133, 8307.
[2] S.Aono and S. Sakaki, J. Phys. Chem. B, **2012**, 116, 13045.
[3] H. Nakano, R. Uchiyama and K. Hirao, J. Comput. Chem., **2002**, 23, 1166.

PIb-20

Electronic Structure of N_2-bridged lanthanide single-molecule magnet

Yue Chen and Shigeyoshi Sakaki
Fukui Institute for Fundamental Chemistry, Kyoto Unviersity
Takano-Nishihiraki-cho, 34-4, Sakyou-ku, Kyoto 606-8103, Japan
e-mail address: sakaki.shigeyoshi.47e@st.kyoto-u.ac.jp

Abstract

Recently, the *f* element complex attracts a lot of interests. One reason is that the *f* elements, with their highly anisotropic magnetic moments, paly important roles in the recent advances in single-molecule magnet. Here, we wish to present the theoretical study on the N_2-bridged lanthanide complex[1] (Scheme 1) because the knowledge of bimetallic system is indispensable for understanding polynuclear systems.

The structure optimized by Broken-Symmetry BHandHLYP functional agrees well with the experimental structure. Both DFT and CASPT2 calculations indicate that the low-spin state (14tet for $[Gd(N_2)Gd]^-$ and 12tet for $[Tb(N_2)Tb]^-$) is more stable than the high-spin state (Table 1). In both $[Gd(N_2)Gd]^-$ and $[Tb(N_2)Tb]^-$, the Mulliken spin density of N_2 are -1.1 in the low-spin state because of the spin polarization (Fig. 1) which is induced by singly occupied low-lying *f* orbitals.

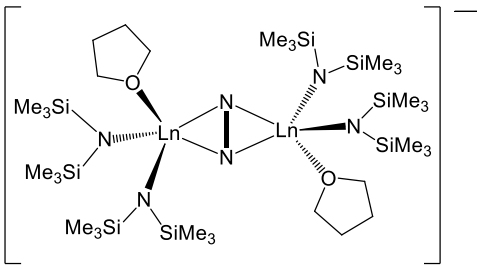

$[Ln(N_2)Ln]^-$
Ln = Gd, Dy

Scheme 1

Table 1. The energies of different spin states

Spin State	DFT	CASPT2
	$[GdN_2Gd]^-$	
16tet	0.0	0.0
14tet	-1.6	-0.8
doublet	-0.8	-
	$[TbN_2Tb]^-$	
14tet	0.0	0.0
12tet	-0.5	-1.7
doublet	0.1	-

a. The doublet state was not calculated by CASPT2

The spin-orbit coupling (SOC) calculated by CASPT2 are 481 and 3553 cm^{-1} in $[Gd(N_2)Gd]^-$ and $[Tb(N_2)Tb]^-$, respectively. Such strong SOC induces a bistable ground state which is responsible for the magnetic properties observed experimentally. In the low-spin state, the singly occupied *f* orbital induces low-spin coupling with the unpaired electron of the negatively charged dinitrogen (N_2^{3-}) interestingly.

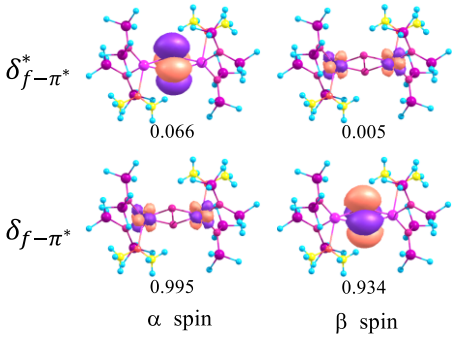

Fig. 1. The spin orbital and occupation number of the δ-type bonding and antibonding orbitals between f orbital and π^* of N_2 moiety.

[1] Rinehart J. D., Fang, Min., Evans, W. J., Long, J. R. *Nat. Chem.* **2011**, *3*, 538-542; *J. Am. Chem. Soc.* 2011, 133,14236-14239.

PIb-21

Large-scale MP2 calculation based on spin-dependent two-component Hamiltonian and divide-and-conquer approach

Masahiko Nakano[1], Junji Seino[1], and Hiromi Nakai[1-4]

[1]*Department of Chemistry and Biochemistry, School of Advanced Science and Engineering, Waseda University, Tokyo 169-8555, Japan*

[2]*Research Institute for Science and Engineering, Waseda University, Tokyo 169-8555, Japan*

[3]*CREST, Japan Science and Technology Agency, 4-1-8 Honcho, Kawaguchi, Saitama 332-0012, Japan*

[4]*Elements Strategy Initiative for Catalysts and Batteries (ESICB), Kyoto University, Katsura, Kyoto 615-8520, Japan*

e-mail address: pico.yokohama@ruri.waseda.jp

I. Introduction

Simultaneous consideration of both relativistic and electron correlation effects is essential to perform accurate electronic-state calculation of heavy element system. However, the practical calculation for large molecules still remains one of the major challenges in quantum chemistry. In this study, we developed the divide-and-conquer (DC)-based [1,2] generalized Hartree-Fock (GHF) and second-order generalized Møller-Plesset perturbation theory (GMP2), which can properly describe spin-orbit interactions derived from the spin-dependent infinite-order Douglas-Kroll-Hess (IODKH) Hamiltonian [3,4].

II. Theory

In the DC-based electron correlation theory, the entire system is spatially divided into disjoint subsystems s. The correlation energy is approximated as the sum of the correlation energy of each subsystem, E_{corr}^{s}. In the case of the DC-GMP2 method, E_{corr}^{s}. is given by

$$E_{\mathrm{corr}}^{s}=\frac{1}{2}\sum_{i^s j^s}^{\{\mathrm{occ}(s)\}}\sum_{a^s b^s}^{\{\mathrm{vir}(s)\}}\sum_{\omega}^{\{\alpha,\beta\}}\sum_{\mu}^{\mathcal{C}(s)}\left(C_{\mu i}^{\omega}\right)^{*}\left(\mu a^{s}\middle|\hat{g}_{ij}\middle|j^{s}b^{s}\right)\left(\tilde{t}_{i^s j^s,a^s b^s}-\tilde{t}_{i^s j^s,b^s a^s}\right) \qquad (1)$$

where $\hat{g}_{ij}$ is the two-electron part of Hamiltonian, C is the molecular orbital (MO) coefficient, $\mathcal{C}(s)$ is the set of atomic orbitals (AOs) in s, and $\tilde{t}_{i^s j^s,a^s b^s}=\left(a^s i^s\middle|\hat{g}_{ij}\middle|b^s j^s\right)/\left(\varepsilon_{i^s}+\varepsilon_{j^s}-\varepsilon_{a^s}-\varepsilon_{b^s}\right)$ is the two-electron excitation amplitude (with ε as an orbital energy). The MO integral in Eq. (1) is calculated by the MO transformation of IODKH-based AO integrals. The local unitary transformation (LUT) scheme [5-7], which exploits the locality of relativistic effects, can be also employed to accelerate the generation of the relativistically transformed AO integrals.

III. Result

Fig. 1 shows the CPU time of (DC-)GHF and (DC-)GMP2 energy calculations for zig-zag chains of $(HF)_n$ using the many-electron LUT-IODKH Hamiltonian with DK3 basis set [8]. This result indicates that the DC scheme achieves linear-scaling, i.e., $\mathcal{O}(N^{1.2})$ and $\mathcal{O}(N^{1.2})$ for GHF and GMP2, respectively.

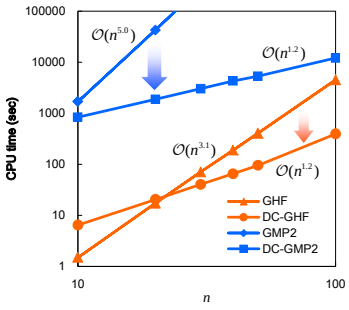

Fig. 1. CPU time of GHF and GMP2 energy calculation for $(HF)_n$ chain with/without DC scheme.

[1] R. Zaleśny, M. G. Papadopoulos, P. G. Mezey, and J. Leszczynski, in *Linear-Scaling Techniques in Computational Chemistry and Physics: Methods and Applications*, (Springer, Dordrecht, 2011), pp.97-127. [2] M. Kobayashi and H. Nakai, *Phys. Chem. Chem. Phys.* **14**, 7629 (2012). [3] M. Barysz and A. J. Sadlej, *J. Chem. Phys.* **116**, 2696 (2002). [4] J. Seino and M. Hada, *Chem. Phys. Lett.* **461**, 327 (2008). [5] J. Seino and H. Nakai, *J. Chem. Phys.* **136**, 244102 (2012). [6] J. Seino and H. Nakai, *J. Chem. Phys.* **137**, 144101 (2012). [7] J. Seino and H. Nakai, *J. Chem. Phys.* **139**, 034109 (2013). [8] T. Tsuchiya, M. Abe, T. Nakajima, and K. Hirao, *J. Chem. Phys.* **115**, 4463 (2001).

PIb-22

An *ab initio* study of nuclear volume effects using 2-compornent relativistic method for isotope fractionation

Keisuke Nemoto[1,3], Minori Abe[1,3], Junji Seino[2,3], Masahiko Hada[1,3]

[1]*Department of Chemistry, Graduate School of Science and Engineering, Tokyo Metropolitan University, 1-1 Minami-Osawa, Hachi-Oji City, Tokyo, 192-0397, Japan,*

[2]*School of advanced science and engineering, Waseda University,* [3]*JST-CREST*

e-mail address: nemoto-keisuke@ed.tmu.ac.jp

Isotope ratio is widely analyzed in geochemistry, cosmochemistry, etc. A general isotopic exchange reaction is described as follows.

A'Y + AX = AY + A'X (A' : light isotope, A : heavy isotope). (1)

In this system, the equilibrium constant α, ([AY]/[A'Y])/([AX]/[A'X]), is always close to 1. Thus the isotope fractionation coefficient ε is conventionally defined as $\alpha-1$. The reason of isotope fractionations is often explained from the vibrational differences caused by isotopic nuclear mass differences. However the molecular vibrational effect can only explain isotope fractionations of light elements. In 1996, experimental results of Fujii *et al*. [1] and a theory of Bigeleisen [2] newly explained a reason of isotope fractionations of heavy elements, so called nuclear volume effect. This effect is caused from electronic state differences due to isotopic difference of nuclear-charge-volume. Nuclear volume term ($\ln K_{nv}$) in ε is described as follows.

$$\ln K_{nv} = (kT)^{-1}\{[E(\mathrm{AX}) - E(\mathrm{A'X})] - [E(\mathrm{AY}) - E(\mathrm{A'Y})]\} \quad (2)$$

Nuclear volume effect is significant in heavy elements and related to electronic state of the nuclear vicinity. Therefore, relativistic effect is very important. Schauble [3] and Abe *et al*. [4] proposed 4-component relativistic calculations of the nuclear volume term. However the 4-component (4c) method is limited to small molecules because of its high computational cost.

Hence in this study, we have calculated the nuclear volume term by various 2-component methods based on the Douglas-Kroll (DK) method to discuss whether they can be alternatives to the 4c method. We have compared the each calculation method to analyze the contribution of higher-order relativistic effect and spin-orbit interaction in $\ln K_{nv}$. Our calculated systems are uranium isotope exchange systems, U(III)-U(IV), and U(IV)-U(VI) with 235 and 238 isotope pairs. Electronic energies of each molecule are obtained using the Gaussian-type finite nucleus model with experimental nuclear charge radii by the DIRAC software.

In our calculations, the spin-dependent infinite-order DK method with mean-field spin-orbit method (IODK+MFSO) provides very close results of $\ln K_{nv}$ to the 4c method less than 1% error. Both the higher-order DK effect and spin-orbit effects are non-negligible for the property of $\ln K_{nv}$. The IODK+MFSO method is much faster than the 4c method, because the number of basis functions is reduced to about one-third. Low computational cost of the IODK+MFSO will pave the way to applications to medium size of molecules (about 50 atoms), which cannot be calculated by the 4c method.

[1] M. Nomura et. al., *J. Am. Chem. Soc.* **118**, 9127 (1996). [2] J. Bigeleisen, *J. Am. Chem. Soc.* **118**, 3676 (1996). [3] E. A. Schauble, *Geochim. Cosmochim. Acta* **71**, 2170 (2007). [4] M. Abe et. al., *J. Chem. Phys.* **129**, 164309 (2008)

PIb-23

Relativistic corrections for an electron confined by two-dimensional quantum dots

Kyozaburo Takeda[1] and Yasuhiro Tokura[2]

[1]*Waseda University, Tokyo 169-855, Japan*

[2]*University of Tsukuba, Tsukuba 305-8571, Japan*

takeda@waseda.jp

Since the success in manipulating the electron's spin, much attention has been focused on the spin-related phenomena, and ``spintronics'' have opened new avenues of exploration in both science and technology. Nowadays, the plan has been further developed to use spins as qubits in the quantum information and computers.

The Pauli spin-orbit (SO) coupling plays a crucial role in the spin-related phenomena although it originates from the relativistic term in Dirac's equation. Besides Pauli's SO coupling, the Dirac equation causes further relativistic corrections. Those representatives are Darwin's term and mass-velocity (MV) interaction. We here focus on these relativistic terms, and reconsider their influences on the electronic structure, comparing with that by Pauli's SO coupling.

Semiconductor QD is expected to become the reliable system to produce useful devices using the acquired knowledge. Accordingly, we study the electronic structure of an electron confined in a 2D quantum dot (QD) by solving Pauli-Breit equation computationally. We further study the influence of the external electric field on the electronic structure because this feature is basically caused by the external SO interaction and is well-known as Rashba effect. The present calculation demonstrates that the Rashba effect in the typical semiconductor QD causes a sizeable shift to the energy eigenstates on the order of a milli-electron volt whereas the other relativistic corrections of the internal SO interaction, MV coupling and Darwin term amount to a shift in energy eigenstates on the order of less than a micro-electron volts, are largely negligible. The Rashba coupling hybridizes the opposite spin state, and the 2nd-order perturbation approach reveals that this hybridization causes the interstate interference and the curious distribution appears in the spin density in the degenerated state. In the presentation, we will discuss the influence of the *quasi*-2D nature of the QD system.

PIb-24

Theoretical study of atomic and molecular systems using electronic stress tensor density and energy density

Hiroo Nozaki, Kazuhide Ichikawa, Akitomo Tachibana

Department of Micro Engineering, Kyoto University, Kyoto 615-8540, Japan

e-mail address: nozaki.hiro.76e@st.kyoto-u.ac.jp

Abstract

The concepts of electronic stress tensor density and energy density give new viewpoints for conventional ideas in chemistry. The formula of electronic stress tensor density is shown as

$$\tau^{Skl}(\vec{r}) = \frac{\hbar^2}{4m}\sum_i \nu_i \left[\psi_i^*(\vec{r})\frac{\partial^2\psi_i(\vec{r})}{\partial x^k \partial x^l} - \frac{\partial\psi_i^*(\vec{r})}{\partial x^k}\frac{\partial\psi_i(\vec{r})}{\partial x^l} + \frac{\partial^2\psi_i^*(\vec{r})}{\partial x^k \partial x^l}\psi_i(\vec{r}) - \frac{\partial\psi_i^*(\vec{r})}{\partial x^l}\frac{\partial\psi_i(\vec{r})}{\partial x^k}\right]$$

where $\psi_i(\vec{r})$ is *i*th natural orbital and ν_i is its occupation number. And {k, l} = {1, 2, 3}.

In this presentation, we introduce the electronic stress tensor and energy density and other related quantities such as tension density, which are based on quantum field theory, and show their connection to the concepts in chemistry. At first, we show that vector field of the tension density gives boundary surfaces of atoms in a molecule as separatrix of the field. We designate this surface as "Lagrange surface" [1]. The case for a HF molecule is depicted in **Fig.1**.

Also, we show that the Lagrange point, the point between two atoms where the tension density vanishes, can well characterize the chemical bond between them. By using energy density at this Lagrange point, we can define bond order b_ε. In addition, the eigenvalues(we denote them by withλ_i $(i = 1, 2, 3)$ of $\lambda_3 \geq \lambda_2 \geq \lambda_1$.) of the electronic stress tensor at this Lagrange point can characterize types of chemical bonding such as covalent bonding and metallic bonding[2]. **Fig.2** shows differential eigenvalues($\lambda_{D32} \equiv \lambda_3 - \lambda_2$ and $\lambda_{D21} \equiv \lambda_2 - \lambda_1$.) of electronic stress tensor density at Lagrange point of metal clusters and other molecules. The bonds between these semimetal atoms are found to have intermediate nature between covalent and metallic bonds.

Figures

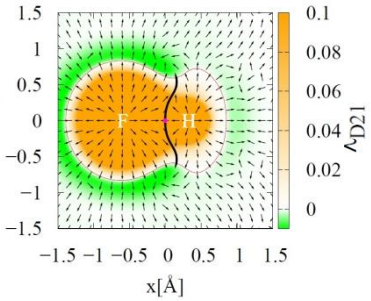

Fig.1

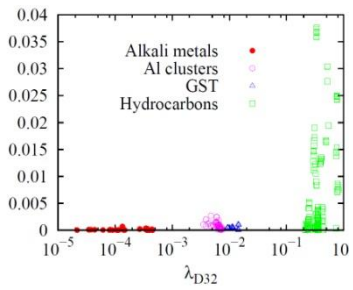

Fig.2

Fig.1 shows tension density and Lagrange surface of HF molecule. The filled circle is the Lagrange point and the thick solid line is the Lagrange surface.

Fig. 2 shows differential eigenvalues at Lagrange point of hydrocarbon(green), metal clusters(red and purple) and GST(blue).

References

[1] A. Tachibana, J. Mol. Struct. (THEOCHEM), **943**, 138 (2010).

[2] K. Ichikawa, H. Nozaki, N. Komazawa and A. Tachibana, AIP Advances **2**, 042195 (2012).

PIb-25

Four-Component Relativistic Occupation Restricted Multi-active Space Self-Consistent Field and its Application to Multireference Perturbation Theory

Satoshi Suzulki, Yoshihiro Watanabe, and Haruyuki Nakano
Department of Chemistry, Graduate School of Sciences, Kyushu University,
6-10-1,Hakozaki, Higashi-ku, Fukuoka 812-8581, Japan
e-mail address: ssuzuki@ccl.scc.kyushu-u.ac.jp

I. Introduction

To elucidate electronic structure of the system including heavy elements, it is essential to take into account both of the relativistic and correlation effects properly. The relativistic effect can be included with four-component Dirac-Hartree-Fock method. Dynamical correlation can be included by post-DHF methods just alike non-relativistic case. Typically, lanthanide or actinide-containing molecules have the open *f* shell and there exit many near-degenerate states. In order to treat near-degenerate states adequately, multireference wavefunction methods are necessary.

In relativistic wavefunction, dimension of multi-configuration self-consistent-field (MCSCF) wavefunction tends to be several times larger than that of nonrelativistic one because of lack of spin symmetry. However, most of the configurations in CASSCF have only small effect to the total wavefunction, and removing these ineffective configurations can reduce the computational cost. One efficient way to remove the ineffective configurations is to divide the active orbital space into several subspaces. We extended occupation restricted multi-active space (ORMAS) method[1], which is a kind of subspace MCSCF/CI, to relativistic wavefunction.

II. Relativistic occupation restricted multi-active space method

In the ORMAS-MCSCF/CI method, the active space is divided into arbitrary numbers of subspaces. Slater determinants to expand MCSCF wavefunction are selected via the minimum and maximum electron occupation numbers in each subspace. In non-relativistic ORMAS method, Slater determinants are represented as a product of alpha and beta strings in order to construct spin eigenfunctions. In our new implementation, in order to describe spin mixed states, a Slater determinant are described as a single string.

We apply relativistic ORMAS-MCSCF wavefunction to multireference perturbation theory. General multiconfiguration perturbation theory (GMC-QDPT)[2,3] is a multistate MRPT based on “general” MCSCF reference function and can be connected to ORMAS-MCSCF function. We calculated excitation energies of several *f*-block and *d*-block elements and $[PtCl_4]^{2-}$. We obtained reasonably accurate results in smaller computational cost.

[1] Ivanic, J., *J.Chem. Phys.* 2003,*119*,9364 [2] Miyajima, M. ; Watanabe, Y.; Nakano, H. *J.Chem. Phys.* 2006,*124*, 044101 [3]Ebisuzaki, R.; Watanabe, Y.; Kawashima, Y.;Nakano, H. *J. Chem. Theory Comput.* 2011, *7*, 998

PIb-26

A highly scalable multireference configuration interaction theory: DMRG-MRCI

Masaaki Saitow, Yuki Kurashige, and Takeshi Yanai
Graduate University for Advanced Studies,
Institute for Molecular Science, 30 Nishigo-Naka,
Myodaiji, Okazaki, Aichi 444-8585, Japan
e-mail address: saitow@ims.ac.jp

I. Introduction

We report the development of the multireference configuration interaction (MRCI) theory that can use much larger active space than has been possible.[1] This has been made possible as a joint approach of the *full-internally contracted* (FIC) representation of the variational basis and the *ab initio* density matrix renormalization group (DMRG) algorithm. The DMRG provides the ability to encode the static correlation in a large active space, while the MRCI describes the crucial correction of the dynamic correlation to the DMRG reference function. The connectivity of the DMRG with the MRCI is provided by use of the FIC representation.

II. Theory

In the earliest FIC-MRCI framework originally developed by Reinsch and Werner,[2] construction of the Hamiltonian of the semi-internal excitation function requires the lengthy 5-rank reduced density matrix (RDM), which hinders the application to the system with a large active space. To eliminate this, we express the semi-internal Hamiltonian element using the multiple commutators;

$$\langle\Psi_0|E^{SI}HE^{'}_{SI}|\Psi_0\rangle = \langle\Psi_0|[E^{SI},[H,E^{'}_{SI}]]|\Psi_0\rangle + E_0\langle\Psi_0|E^{SI}E^{'}_{SI}|\Psi_0\rangle$$

where Ψ_0 and E_{SI} represent the reference function and the semi-internal excitation operator, respectively. The 5-RDM is cancelled out in the first term on the right-hand side without any approximations. In addition, we use the cumulant-approximation to the 4-RDM. As a consequence, construction of the Hamiltonian requires only 1-3 RDMs. Nevertheless, the working equation of DMRG-MRCI is composed of exceedingly complicated tensor contractions. To address this complexity, we have developed the tensor generator, which expands the many-body ansatz according to the Wick's theorem and generates the parallelized tensor contraction codes.[3] The DMRG-MRCI program is implemented in the Orz suite, our in-house quantum chemistry program, and will be released under the open-source license.

[1] M. Saitow, Y. Kurashige, and T. Yanai, J. Chem. Phys. **139**, 044118 (2013).
[2] H.-J. Werner, and E.A. Reinsch, J. Chem. Phys. **76**, 3144 (1982).
[3] M. Saitow, FEMTO :: An Integrated Toolset for the Automated Tensor Generation (https://github.com/msaitow)

PIb-27

DMRG CAS-SI employing flexible nuclear screening spin-orbit approximation

Jakub Chalupský, Yuki Kurashige, and Takeshi Yanai
Department of Theoretical and Computational Molecular Science, Institute for Molecular Science, Okazaki, Aichi 444-8585
e-mail address: jakub@ims.ac.jp

We present a new implementation of complete active space state interaction (CAS-SI) method. [1] Unlike most of the existing implementations, our quantum chemistry package named ORZ can use not only conventional full-CI CASSCF wave functions, but also CASSCF wave functions based on density matrix renormalization group theory (DMRG). [2] DMRG allows us to use size of active space beyond the limit of conventional CASSCF, recently also for calculation of transition matrix elements and subsequent quasi-degenerate perturbation theory (QDPT) calculations.

Along with DMRG/full-CI CAS-SI approach, we use accurate and highly efficient approximation to the two-electron spin-orbit coupling (SOC) terms developed recently, which we call flexible nuclear screening spin-orbit (FNSSO). [3] This approximation uses an effective one-electron SOC operator and accounts for the effect of two-electron SOC by screening the nuclear charges involved in the corresponding one-electron SOC integrals (i.e., only one-electron integrals have to be evaluated explicitly). The screening is based on a highly flexible scheme, which uses mostly atomic *ab initio* parameters, and thus allows for accurate description of SOC (see Table 1) with minimal computational cost.

Performance of the presented methodology is discussed on practical examples, involving molecules composed of atoms from the lightest to the heaviest.

Table 1: Magnitude of SOC matrix elements (in cm^{-1}) calculated at DKH1 level with exact (SO_{full}) and various approximate treatments of two-electron SOC, using CASSCF wave functions and ANO-RCC basis set, and percentage error (PE) of used approximate approaches.

	states	SO_{full}	SO_{MF}	PE	AMFI	PE	SNSO	PE	FNSSO	PE
CH_2	S_0/T_1	10.9	11.0	0.2	11.0	0.3	14.0	28.1	11.0	1.0
GeH_2	S_0/T_1	391.9	392.0	0.0	391.6	−0.1	411.8	5.1	391.7	0.0
PbH_2	S_0/T_1	3310.4	3310.4	0.0	3309.9	0.0	3368.7	1.8	3316.5	0.2
H_2O_2	S_0/T_1	41.1	40.9	−0.5	42.0	2.1	47.2	14.7	40.9	−0.5
H_2Se_2	S_0/T_1	784.6	784.6	0.0	785.3	0.1	818.4	4.3	784.2	0.0
H_2Po_2	S_0/T_1	5225.9	5225.9	0.0	5228.7	0.1	5309.0	1.6	5235.2	0.2
CO^+	D_1/D_2	18.1	18.2	0.5	17.0	−6.3	19.9	9.7	17.8	−1.7
	D_2/D_3	60.3	60.1	−0.4	58.0	−3.8	69.8	15.7	59.7	−1.0
NO	D_1/D_2	62.6	62.9	0.4	66.4	6.0	74.7	19.3	64.1	2.3
$[Fe(H_2O)_6]^{3+}$	D_1/D_2	235.7	235.4	−0.1	228.5	−3.1	252.6	7.2	228.3	−3.2
$[Ru(H_2O)_6]^{3+}$	D_1/D_2	553.8	553.7	0.0	550.9	−0.5	595.0	7.4	551.5	−0.4
$[Os(H_2O)_6]^{3+}$	D_1/D_2	1805.1	1805.0	0.0	1799.4	−0.3	1901.9	5.4	1802.2	−0.2
NdO_2	T_1/T_2	2442.3	2468.1	1.1	2438.5	−0.2	2691.7	10.2	2459.0	0.7
UO_2	T_1/T_2	3005.1	3006.0	0.0	2977.3	−0.9	3246.9	8.0	3001.9	−0.1

[1] P.-Å. Malmqvist, B. O. Roos, and B. Schimmelpfennig, *Chem. Phys. Lett.* **357**, 230 (2002).
[2] K. G. Wilson, *Rev. Mod. Phys.* **47**, 773 (1975); S. R. White, *Phys. Rev. Lett.* **69**, 2863 (1992).
[3] J. Chalupský, and T. Yanai, *J. Chem. Phys.* accepted.

PIb-28

Chemically intuitive indices for charge-transfer excitation based on SAC-CI and TD-DFT calculations

Masahiro Ehara, Ryoichi Fukuda, Carlo Adamo, and Ilaria Ciofini
Institute for Molecular Science,
Myodaiji Nishigonaka 38, Okazaki 444-8585 Japan
e-mail address: ehara@ims.ac.jp

A recently proposed charge-transfer (CT) index and some related quantities aimed to the description of CT excitations in push-pull donor-acceptor model systems were computed in vacuum and in ethanol by the direct SAC-CI method including solvent effects by means of the nonequilibrium state-specific approach. The D-A molecular system (Fig. 1) was analyzed by the SAC/SAC-CI electron density difference between ground and excited states with calculating CT indexes (Fig. 2). The effects of both solvation and electron correlations on these quantities were found to be significant (Table 1). The present results are also in line with previous TD-DFT calculations and they demonstrate that SAC-CI provides a description of the excitation character close to that of TD-PBE0. Indeed, CT indices evaluated by the SAC-CI and TD-PBE0 would be useful in the field of materials chemistry, for the design and development of novel molecular materials.

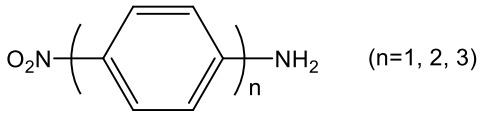

Fig. 1. α,ω-nitro, amino-polyphenylenes studied in the present work

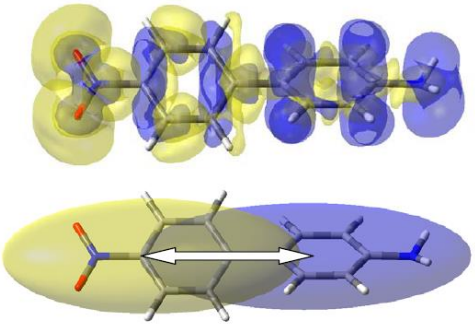

Fig. 2. Difference of the SAC/SAC-CI electron density between ground and excited states of P2 in ethanol.

Table 1. Calculated CT indices (Å) for Pn systems (n=1 to 3)

	P1			P2			P3		
	D_{CT}	H	t	D_{CT}	H	t	D_{CT}	H	t
SAC-CI (in ethanol)	2.97	2.00	0.97	4.86	3.11	1.75	6.06	4.14	1.92
SAC-CI (in vacuum)	0.49	1.31	-0.98	3.60	3.08	0.52	4.29	4.12	0.17
PBE0[a] (in ethanol)	2.6	2.0	0.6	5.0	3.1	1.9	5.9	4.0	1.9
LC-PBE[a] (in ethanol)	2.5	2.0	0.5	3.7	3.2	0.5	3.8	4.2	-0.4
CIS[a] (in ethanol)	2.1	2.0	0.1	3.0	3.0	0.0	3.8	4.2	-0.4

[1] M. Ehara, R. Fukuda, C. Adamo, I. Ciofini, *J. Comp. Chem.* **2013**, 34, 2498.
[2] T. Le Bahers, C. Adamo, I. Ciofini, *J. Chem. Theor. Comput.* **2011**, *7*, 2498.

PIb-29

General Coalescence Conditions for the Exact Wave Functions: Higher-Order Relations for Many-Particle Systems

Yusaku I. Kurokawa, Hiroyuki Nakashima, and Hiroshi Nakatsuji
Quantum Chemistry Research Institute
Kyodai Katsura Venture Plaza 107, Goryo Oohara 1-36, Nishikyo-ku, Kyoto 615-8245, Japan
e-mail address: y_kurokawa @qcri.or.jp

The coalescence region, where two charged particles come very close to each other, is a special region in molecular quantum mechanics because it is a singular point of the Coulombic potential in the Hamiltonian $\hat{H}$ of the Schrödinger equation (SE), $\left(\hat{H}-E\right)\psi=0$.

In the previous study, we derived an infinite number of necessary conditions that must be satisfied at a coalescence (cusp) point by the non-relativistic time-independent exact wave functions for two-particle systems [1]. Some of these conditions are known to be Kato's cusp condition (CC) and Rassolov and Chipman's CC. In the present study, we extended those conditions to many-particle systems [2]. These are called generalized coalescence conditions (GCCs), and Kato's CC and Rassolov and Chipman's CC are included in these conditions. GCCs can be applied not only to Coulombic systems but also to any system in which the interaction between two particles is represented in a power series of inter-particle distances.

For example, the second order GCC for the helium atom in the electron-electron (e-e) coalescence situation is written as

$$F_{00}^{(2)} \equiv f_{00}^{(5)} - \tfrac{23}{90} f_{00}^{(4)} + \tfrac{53}{180} f_{00}^{(3)} - \tfrac{13}{144} f_{00}^{(2)} + \tfrac{1}{18} f_{00}^{(1)} - \tfrac{1}{45} f_{00}^{(0)} = 0 \quad ,$$

where we assume that the coalescence point is distant from the nucleus by 1 a.u.

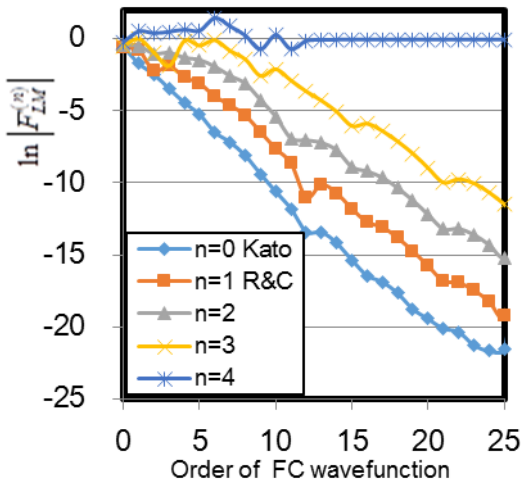

Fig. Logarithmic plot of the electron-electron coalescence values F of the FC wave functions of the helium atom in the ground state. "n" represents the order of the coalescence values. The x-axis represents the order of the FC wave function, *i.e.*, the accuracy of the wave function.

We confirmed the correctness of our derivation of these GCCs by applying the exact wave function of a harmonium in e-e and e-n coalescence situations. In addition, we applied the free complement (FC) wave functions[3-6] of a helium atom to the GCCs to examine the accuracy of the FC wave function in the context of a coalescence situation (see Fig).

[1] Y. I. Kurokawa, H. Nakashima, and H. Nakatsuji, J. Chem. Phys. **139**, 044114-1 (2013) [2] to be submitted in JCP [3] H. Nakatsuji, J. Chem. Phys. **113**, 2949 (2000). [4] H. Nakatsuji, Phys. Rev. Lett. **93**, 030403 (2004) [5] H. Nakatsuji, H. Nakashima, Y. Kurokawa, A. Ishikawa, Phys. Rev. Lett. **99**, 240402 (2007) [6] H. Nakatsuji, Acc. Chem. Res., **45**, 1480-1490 (2012)

PIb-30

Free Complement Calculations of the Helium atom: Gaussian versus Slater

Johanna Langner[1,2] and Hiroshi Nakatsuji[1]

[1]*Quantum Chemistry Research Institute, Katsura, Nishikyou-ku, Kyoto 615-8510, Japan*
[2]*Universität Leipzig, Fakultät für Chemie und Mineralogie, Johannisallee 29, D-04103 Leipzig, Germany*
e-mail address: jlangner@qcri.or.jp

The free complement method[1][2][3] for generating the exact wave function from an approximate initial wave function has been applied to the helium atom starting from the Gaussian function $\psi_0 = \exp\left(-\alpha r^2\right)$. The exponential parameter α has been optimized. The results have been compared to earlier calculations starting from a Slater initial function[4] with respect to the accuracy of the obtained energy, the trends in α as well as properties of the wave function.

Table 1. *Energy and optimized α of first orders with Gaussian initial function*

Order	M_n	Optimal α	Energy	# Correct Digits
0	1	0.7670	**-2**.30098699313	0.7
1	6	0.8344	**-2**.78432756866	1.4
2	27	0.5143	**-2.90**011978328	2.9
3	71	0.3963	**-2.903**64267430	4.6
4	151	0.3329	**-2.90372**005676	5.8
5	273	0.3164	**-2.903723**97090	6.9
6	450	0.3120	**-2.9037243**1688	7.7
7	688	0.3125	**-2.9037243**6586	8.4
8	1000	0.3143	**-2.9037243**7452	9.1
Exact			-2.903724377030	

A comparison of the accuracy of the results given in Table 1 to the ones from the corresponding calculation using Slater-type functions, as published in [4], is shown in Table 2.

Table 2. *Comparison of number of correct digits using Gaussian- vs. Slater-type functions*

Order	M_n		# of correct digits	
	Gaussian	Slater	Gaussian	Slater
0	1	1	0.7	1.7
1	6	3	1.4	2.4
2	27	7	2.9	4.0
3	71	13	4.6	4.5
4	151	22	5.8	5.4
5	273	34	6.9	5.9
6	450	50	7.7	6.6
7	688	70	8.4	7.0
8	1000	95	9.1	7.6

The energies calculated with Gaussian functions are less accurate than the Slater-type ones up to order three, but get more accurate with higher orders. This is likely due to the number of complement functions M_n rising much faster when using Gaussian-type functions, exceeding ten times of the number of complement functions in the Slater calculation at order 8. In order to achieve a given accuracy, the number of necessary Gaussian-type complement functions is generally over four times larger than the number of required Slater-type complement functions. We will compare on other properties like cusp value, local energy, etc. between Slater and Gaussian calculations.

[1] - H. Nakatsuji, J. Chem. Phys., **113**, 2949-2956 (2000).
[2] - H. Nakatsuji, Phys. Rev. A, **72**, 062110 (2005).
[3] - H. Nakatsuji, Acc. Chem. Res., **45**, 1480-1490 (2012).
[4] - H. Nakashima, H. Nakatsuji, J. Chem. Phys. **127**, 224104-1-14 (2007)

PIb-31

Theoretical chiral molecular technology, ChiraSac applied to biological molecules

Tomoo Miyahara and Hiroshi Nakatsuji
Quantum Chemistry Research Institute (QCRI), Katsura, Nishikyou-ku, Kyoto 615-8510, Japan
e-mail: t.miyahara@qcri.or.jp

I. Introduction

Circular dichroism (CD) spectra are sensitive to low-energy processes like the rotations around the single bonds and to weak interactions like hydrogen-bonding and stacking. If we use a reliable method, we can understand each peak of the CD spectra. The SAC-CI method, one of the most reliable excited-state theories, is useful for analyzing the CD spectra [1-4]. Therefore, using the SAC-CI method and many other useful theoretical methods included in Gaussian 09[5], we have undertaken a high-reliable molecular technology, ChiraSac, for the structural analysis and functional creation of chiral molecules [6]. In this study, we apply it to biological molecules.

II. Computational details

We optimized the geometries of estradiol – estrogen receptor complex by the QM (B3LYP) / MM (Amber) method and calculated their CD spectra by the SAC-CI method.

III. Results and discussion

As shown in right Figure, the small models (A and B) were strongly affected by the MM charge. But, using the large models C or D that include important amino acids around estradiol, we obtained highly reliable results. We also applied to the CD spectra of rhodopsin isomerization.

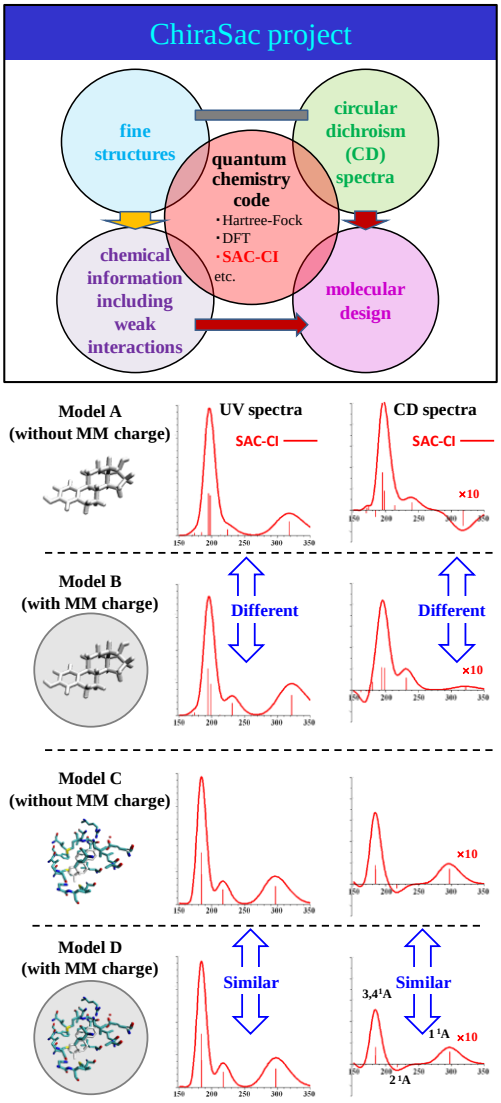

Model	QM (SAC-CI)	QM (Hartree-Fock)	MM (Amber)
A	Estradiol	None	None
B	Estradiol	None	All amino acids
C	Estradiol	18 amino acids	None
D	Estradiol	18 amino acids	Other amino acids

[1] H. Nakatsuji, K. Hirao, J. Chem. Phys. 1978, 68, 2053, H. Nakatsuji, Chem. Phys. Lett.1978, 59, 362.; 1979, 67, 329, 334; Bull. Chem. Soc. Jap. 2005, 78, 1705. [2] M. Ehara, J. Hasegawa, H. Nakatsuji, Theory and applications of Computational Chemistry, The First 40 Years, Elsevier Oxford, 2005; p1099. [3] SAC-CI homepage. http://www.qcri.or.jp/sacci/ (16/12/2012). [4] T. Miyahara, H. Nakatsuji, H. Sugiyama, J. Phys. Chem. A, 117, 42 (2013). [5] M. J. Frisch, et at. GAUSSIAN 03, Gaussian, Inc. Pittsburgh PA, 2003. [6] T. Miyahara, H. Nakatsuji, J. Phys. Chem. A, in press.